Millimeter-wave antenna noise temperature due to rain clouds: theoretical model and statistical prediction

Frank Silvio Marzano [1,2], Mario Montopoli [2]

[1] *DIE, Sapienza University of Rome*
Via Eudossiana, 18, 00184 Rome, Italy
[1] marzano@die.uniroma1.it

[2] *DIEI and CETEMPS, University of L'Aquila*
Poggio di Roio, 67040 L'Aquila, Italy
[2] mmontop@ing.univaq.it

***Abstract*— Model-oriented methods to predict antenna noise temperature due to rainfall along slant paths are developed and illustrated for communication systems at Ka band and above. The adopted Sky Noise Eddington Model (SNEM) relies on an accurate analytical solution of the radiative transfer equation and on stratiform and convective rainfall stratified structures, synthetically generated from cloud-resolving model statistics. The approach to predict antenna noise temperature is based on the multiple regression analysis, trained by SNEM-derived cloud radiative datasets. In order to test the proposed prediction technique, measurements of the ITALSAT satellite ground-station at Pomezia (Rome, Italy) are taken into consideration for 2 case studies. Combined data from the ITALSAT three-beacon receiver at 18.7, 39.6 and 49.5 GHz and from a three-channel microwave radiometer at 13.0, 23.8 and 31.6 GHz are processed and discussed.**

I. INTRODUCTION

The optimal allocation of channel resources above Ku band is limited by the significant impact of radio-meteorological factors which can irremediably degrade the quality of service for fairly high percentage of time [1]-[3]. The major cause of outages at Ka band and above is not only convective rainfall, as for lower frequencies, but even non-precipitating clouds and moderate precipitation produced by stratiform clouds [4]-[6]. Channel characterization and modeling above Ku band may be extremely important for very small aperture terminals (VSAT's), for point-to-multipoint networks and in, in general, for low-fade margin systems [7]. For small carrier-to-noise (C/N) ratio, the system equivalent noise temperature decreases and the impact of atmospheric noise temperature can become non-negligible [9]. An appealing goal for designing purposes could be to predict antenna noise temperature due to rain clouds in an adaptive mode, and possibly on short to medium time scales, from measurements of path attenuation or from available meteorological data [10],[11].

Simplified empirical-statistical prediction models of radio-meteorological effects are not always suitable when extrapolated to short-term time scales and to millimeter-wave frequencies [12]. Experimental characterization of atmospheric radio-propagation effects along satellite links is of major importance for model testing, but it is very often unfeasible and costly (e.g., [13]-[14]).The alternative choice is to adopt a physical approach to the modeling of atmospheric fade, noise and dynamics [15]. Even though subject to the validity domain of the model itself, the physical approach can offer a thorough insight into radio-wave propagation trough atmosphere (e.g., [16]). Hydrometeor multiple scattering should be taken into account when incoherent effects due to rain and ice multiple scattering are involved, especially at frequencies at Ka band and above [17].

The increasing use of co-located microwave radiometers in synergy with satellite beacon receivers has renewed the interest in measuring and modeling the sky-noise antenna temperature. A previous work was devoted to set up a rigorous simplified theoretical framework for describing antenna noise temperature and to propose radiative models of clouds and rainfall [18]. The antenna noise temperature was analytically expressed by resorting to the sky-noise Eddington model solution of the radiative transfer equation for plane-parallel atmosphere geometry. Physical-statistical stratified models of clouds and rainfall were also described in terms of antenna noise temperature signatures.

The present work is aimed at exploiting these physically-oriented rain-cloud radiative models to: i) show the limitation of assuming a constant value for the mean radiative (or effective) temperature T_m; ii) predict T_m due to convective and stratiform rainfall from either path attenuation or rain rate measurements; iii) test the physically-oriented prediction methods with available satellite-link data at Ka band and above.

II. MODELING RAINFALL ANTENNA NOISE TEMPERATURE

For ground-based measurements of sky noise antenna temperature within a vertically-stratified atmosphere, it is convenient to express the received brightness temperature T_B through the *effective mean (radiative) temperature* T_m [15]:

$$\begin{aligned} T_B(z=0,\theta) &= T_m(z=0,\theta)\left(1-e^{-\tau/\mu_0}\right)+T_c e^{-\tau/\mu_0} = \\ &= T_m(z=0,\theta)\left(1-10^{-A}\right)+T_c 10^{-A} \cong T_A(z=0,\theta) \end{aligned} \quad (1)$$

where z=0 stands for surface height, τ is the vertical optical thickness (due to both absorption and scattering), μ_0=cosθ with θ the observation zenith angle, A the slant-path attenuation (with A=4.343τ/μ_0 in decibels), and T_c the microwave cosmic T_B (with $T_c \cong$2.73 K). Note that both T_m and τ by definition depend on frequency and hydrometeor content on their turn. The impact of the antenna radiation pattern is generally less than 0.5% in rainy conditions so that we can substitute the antenna noise temperature T_A with the brightness temperature T_B, as in the last term of (1) [18]. By inverting (1), we can derive the following definition for T_m:

$$T_m(z=0,\theta) \equiv \frac{T_B(z=0,\theta) - T_c e^{-\tau/\mu_0}}{1 - e^{-\tau/\mu_0}} \quad (2)$$

It is apparent from (2) that T_m does not necessarily coincide with the thermodynamic temperature of the atmosphere, but takes into account, in a frequency-dependent way, both radiative and observation parameters. From (2) the atmospheric slant-path attenuation A can be also derived from T_m and radiometric measurements of T_B:

$$A(z=0,\theta) = \frac{4.343}{\mu_0}\tau = \ln\left(\frac{T_m(z=0,\theta) - T_c}{T_m(z=0,\theta) - T_B(z=0,\theta)}\right) \quad (3)$$

In order to handle (1) and (3) using only either A or T_B measurements, respectively, a simple way is to resort to the ITU-R approximate model [12]. The latter is such that T_m is supposed to be constant:

$$T_m(z=0,\theta,\nu) = T_0 \quad (4)$$

where the value $T_0 \cong$275 K is suggested [16].

Indeed, (4) is a very crude approximation for T_m. To realize it, we can consider the general theoretical framework of the Sky Noise Eddington Model (SNEM), extensively described in [18]. The basic assumption of SNEM is to expand $T_B(z,\theta)$ in terms of Legendre polynomials (with respect to μ=cosθ) up to the first order, deriving the expansion coefficients from the solution of the radiative transfer integro-differential equation [18]. In case of a homogeneous atmospheric slab with τ equals to the total optical thickness (τ_s) and a temperature linear decrement, it is quite straightforward to derive the following closed-form expression for the ground-based effective mean temperature:

$$T_m(z=0,\theta) = \left[t_0 - t_1\mu_0 - \frac{wg\mu_0}{(1-wg)}t_1\right] + \frac{1}{1-e^{-\tau_s/\mu}}\left[t_1\tau_s - wC_1\frac{1+c\mu_0 g}{1-\lambda\mu_0}(e^{-\tau_s/\mu_0} - e^{-\lambda\tau_s}) + \right. \quad (5)$$
$$\left. - wC_2\frac{1-c\mu_0 g}{1+\lambda\mu_0}(e^{-\tau_s/\mu_0} - e^{\lambda\tau_s})\right]$$

where C_1 and C_2 are the integration constants, derived from the imposition of the boundary conditions, t_0 and t_1 are the temperature decrease intercept and slope (with respect to the optical thickness τ), respectively. The quantity λ is a known eigenvalue, expressed in terms of volumetric albedo w (i.e., scattering over extinction coefficient) and the scattering asymmetry factor g [18]. Overall errors of (5) have been found to be less than 1% when compared to fully-numerical solutions of the radiative transfer equation. Previous results in (5) can be generalized to an inhomogeneous planar atmosphere by adopting a recursive approach [18].

If the albedo w is zero in (5) (i.e., the atmosphere is not scattering), then T_m can be expressed as:

$$T_m(z=0,\theta) = \left[t_0 - t_1\mu_0\right] + \left[\frac{t_1\tau_s}{1-e^{-\tau_s/\mu_0}}\right] \quad (6)$$

Finally, in case of thermally uniform non-scattering slab at temperature T_0, then it results: $t_0=T_0$, t_1=0, w=0 and g=0. Then, from (6) we can derive the approximate formula (4), i.e.: $T_m(z=0,\theta)=T_0$. Previous considerations may give a hint on the theoretical validity of the ITU-R atmospheric sky-noise model, given in (4).

III. Predicting Antenna Noise Temperature

Synthetic cloud radiative datasets, generated by SNEM, can be used for developing physically-oriented statistical prediction techniques. Within this simulation environment, we can perform such analysis by assuming that the random variability of the radiopropagation process through a rain cloud is well (and realistically) represented by the synthetic radiopropagation data set [18]. As already mentioned, these results would be generally valid only for environmental conditions and antenna configurations assumed within the model itself, but this would be similarly true for a specific experimental analysis as well. More importantly, the synthetic data set offers several parameters to be tuned to a given measuring station.

In order to set up a model-based statistical predictor, we may assume to have, as inputs, different sets of parameters: i) path attenuation $A(\nu,\theta)$ at given frequency ν and angle θ, available from ground-based receiver measurements; ii) measured surface rain rate R, available from rain-gauge or disdrometer measurements; iii) columnar liquid water content L, available either from meteorological forecast numerical model outputs or from ground-based radiometer measurements. A combination of the previous parameters can be also taken into consideration within a measured predictor vector $\mathbf{x}$ [19].The statistical predictor can be designed as an algorithm with two successive stages. First of all, we can identify the observed meteorological situation, e.g., in terms of clear, cloudy or rainy condition. Then, we can estimate the radiopropagation parameter of interest, such as T_m.

A way to approach the problem of rain class recognition is to resort to the maximum likelihood (ML) technique by assuming a multi-dimensional Gaussian metrics for the difference between the measured quantities, expressed by a vector $\mathbf{x}$, and their known mean value or centroids $\langle\mathbf{x}_c\rangle$. Thus, the first ML stage consists in maximizing a proper norm or distance function $d(c)$ with respect to the class c [19]:

$$\hat{c} = ML_c\left[d(c)\right] = ML_c\left[-\sqrt{\left(\mathbf{x}- < \mathbf{x}_c >\right)^T \left[\mathbf{C}_{xc}\right]^{-1}\left(\mathbf{x}- < \mathbf{x}_c >\right)}\right] \quad (7)$$

where c may be equal to Ca (clear air), Cl (non-precipitating clouds), Ns (nimbostratus) or Cb (cumulonimbus). The matrices $\mathbf{C}_{xc}$ are the class auto-covariance matrices of each class c. The superscripts "T" and "-1" indicate matrix transpose and inversion, respectively, whereas ML_c is a functional which returns the value of c corresponding to the maximum of $d(c)$.

Once rain conditions have been identified, we can proceed to predict the sky noise effective mean temperature. A non-linear regression approach has been chosen here by adopting a polynomial model. Regression techniques are fairly well suited to this aim as they are both simple to handle and can be generalized in order to perform a robust estimation in presence of unexpected noise and errors [19]. For ground-based antennas, the prediction models of T_m can be stated in different manners, e.g. with respect to predictors A, L or R belonging to an estimated class c [19]:

$$\begin{cases} \hat{T}_m(z=0,\theta,\nu;\hat{c}) = a_0 + \sum_{j=1}^{J}\left\{\sum_{k=1}^{K} a_{jk}\left[A(\theta,\nu_k;\hat{c})\right]^j\right\} \\ \hat{T}_m(z=0,\theta,\nu;\hat{c}) = b_0 + \sum_{l=1}^{L} b_l\left[L(\hat{c})\right]^l \\ \hat{T}_m(z=0,\theta,\nu;\hat{c}) = d_0 + \sum_{n=1}^{N} d_n\left[R(\hat{c})\right]^n \end{cases} \quad (8)$$

where ν_k is the k-th frequency and J, L and N are the polynomial maximum orders. The following units hold for (8): T_m [K], A [dB], L [kg·m^{-2}] and R [mm·h^{-1}]. The previous formulas can be easily extended to a combination of the available predictors. If K=1, (8) reduces to an estimate of T_m using the co-frequency path attenuation.

The coefficients are dependent on the observation angle and frequency. They can be estimated by employing again the SNEM-derived cloud radiative dataset, previously described. To this aim, we have divided the mid-season dataset into a train and test set, adding to simulated T_A's a Gaussian noise with a zero mean and a standard deviation equal to 1 K. For K=1 and $\nu=\nu_1$, polynomial regression models with various J, L and N have been compared to power-law relations in terms of root mean square errors (RMSE's). The output of this optimization procedure has suggested the choice of a cubic function (i.e., J=3, L=3 and N=3) for all 3 models in (8).

The obtained coefficients in (8) are reported in Table I for Ns and Cb clouds and at 18.7 and 39.6 GHz and for 45° elevation angle, as an example. The analysis of the Table RMSE's confirms what already noted: i) the effective mean temperature is highly correlated with path attenuation and this provides a fairly accurate prediction; ii) saturation effects for A-T_m are responsible for larger errors at 39.7 GHz in case of high rain rates; iii) estimates of T_m are less accurate when using R as a predictor since R is poorly correlated with T_m. The last comment can be further deepened by noting that R is a near-surface parameter, whereas both A and L are vertically-integrated parameters highly correlated to T_A, and then T_m, measurements.

TABLE I. Cubic regression coefficients of (8) for Ns and Cb at 18.7 and 39.6 GHz at 45° for a mid-season dataset together with root means square errors (RMSE's), given in [K]. Results for Cb are valid for R>10 mm/h.

T_m [K]	Ns		Cb	
	18.7 GHz	39.6 GHz	18.7 GHz	39.6 GHz
a_0	72.9647	64.6964	106.7186	225.4640
a_{11}	14.6261	28.9851	19.1822	3.4444
a_{21}	5.7085	-1.0800	-0.6556	-0.0542
a_{31}	-0.9146	0.0031	0.0072	0.0003
RMSE	2.7	4.7	6.0	11.8
b_0	75.6557	74.4539	29.8581	205.2246
b_1	22.3167	127.2115	124.8401	51.4969
b_2	0.4230	-23.1472	-19.7491	-9.4235
b_3	0.4132	0.7121	1.0211	0.5415
RMSE	6.2	17.7	11.6	11.5
d_0	82.2646	110.5684	106.2583	237.9072
d_1	4.7295	22.0927	9.5560	3.5984
d_2	-0.3004	-1.6542	-0.1647	-0.0726
d_3	0.0328	0.0728	0.0009	0.0005
RMSE	8.7	28.5	18.4	13.5

IV. USING EXPERIMENTAL SATELLITE-LINK DATA

Path-attenuation data acquired at the ITALSAT-satellite ground-station located in Pomezia (Rome, Italy) have been used in this work [8]. Since April 1994 and till January 2004, measurements of the three ITALSAT-F1 propagation beacons at 18.7, 39.6, and 49.5 GHz have been performed every second at an elevation angle of 41.8° with a receiver-antenna of 3.5 m (i.e., beam-widths from 0.2° to 0.5°). The ground station has measured the amplitude and phase of copolar and crosspolar signals at 18.7 and 39.6 GHz, and the polarization transfer matrix at 49.5 GHz.

Concurrent measurements, performed by two microwave ground-based radiometers (named REC-1 and REC-2) both pointed to the ITALSAT satellite, have been synchronously logged every 4 seconds by the ITALSAT ground station together with a set of surface meteorological instruments. Radio-sounding meteorological profiles have been also available twice a day with the balloons launched 5 km from the ITALSAT ground-station. The radiometer, called REC-2, is a dual-channel system at 23.8 and 31.6 GHz. It consists of a dual channel offset-fed reflector antenna with a beam-width of about 1.8° and 1.9° at 23.8 and 31.6 GHz, respectively. Heated air blows across the reflector, preventing the formation of the dew and accumulation of light drizzle, snow, or hail on the reflector surface. The radiometer calibration has been carried out by means of the tipping-curve method. The expected overall radiometric accuracy is about 1 K. The single channel radiometer called REC-1 is an independent system operating at 13.0 GHz. This radiometer has basically the same characteristics of the REC-2 system, but with a larger reflector antenna providing a beam-width of about 3.5°.

A. ITALSAT case studies

In order to show some examples, we have selected a case of moderate rainfall, observed during April 29, 1998. A

moving average with 1-minute window and 1-minute sampling period has been applied to analyze raw data of ITALSAT-station instrumentation.

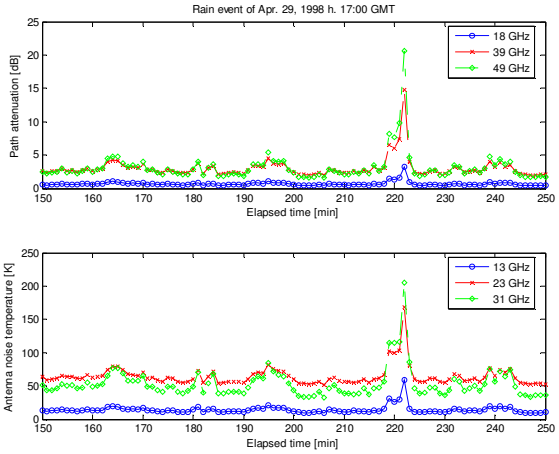

Fig. 1. Slant path attenuation (top panel) at 18.7, 39.6 and 49.5 GHz and brightness temperatures (bottom panel) at 13.0, 23.8 and 31.6 GHz, measured by a beacon receiver and microwave radiometer at 41.8° at the ITALSAT receiving station in Pomezia (Rome, Italy) on April 29, 1998.

The case study refers to a moderate rainfall event. Fig. 1 shows the slant path attenuation A at 18.7, 39.6 and 49.5 GHz and antenna noise temperature T_A at 13.0, 23.8 and 31.6 GHz, measured by the beacon receiver and ground-based radiometer at 41.8° elevation angle on April 29, 1998 at 17:00 GMT for about 2 hours. The event evolution shows path-attenuations and sky-noise temperatures always below 5 dB and 90 K, respectively, expect around the minute 220 where both A and T_A exhibit a peak at all frequencies. At 18.7 GHz path attenuation reaches about 5 dB, whereas at 49.5 GHz values up to 20 dB are measured. Radiometric data range from about 55 K, measured at 13 GHz, to about 200 K at 31.6 GHz. This microwave signature is typical of cloudy and stratiform rainfall scenario with an embedded more intense episode, probably due to localized convective activity around the minute 220.

B. Antenna noise prediction from path attenuation

In order to apply the proposed physically-oriented prediction technique, the first step is to classify the rainfall regime of each time step in an automatic way by using (7). In our experimental context, we can set the observation vector **x** as the combination of the 3 ITALSAT measured co-polar attenuations, i.e.: $\mathbf{x}=[A(\theta,\nu_{18}), A(\theta,\nu_{39}), A(\theta,\nu_{49})]^T$.

To get a qualitative appraisal of the ML classification method, for the case study of April 29, 1998 Fig. 2 shows a comparison between measured and simulated antenna noise temperatures at 13.0 and 23.8 GHz and path attenuations at 18.7 and 39.6 GHz. Centroids of Ca, Cl, Ns and Cb classes are also superimposed, as derived from Table I but at 41.8° elevation. Even though the classification is carried out in a 4-D hyperspace, the figure clearly shows the membership of the rain event which is basically stratiform.

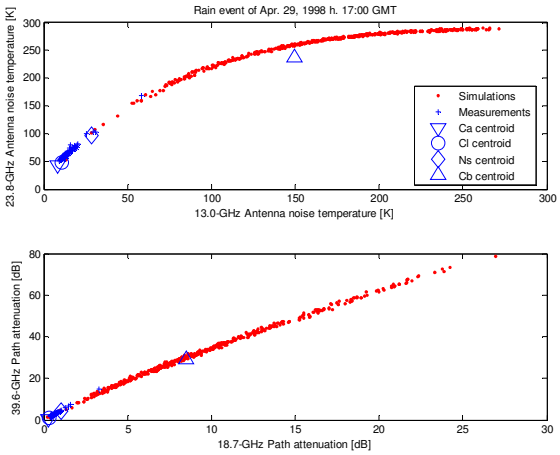

Fig. 2. Comparison between measured and simulated antenna noise temperature (top panels) at 13.0 and 23.8 GHz and path attenuation (bottom panels) at 18.7 and 39.6 GHz for an elevation of 41.8°. Centroids of simulated clear-air (Cl), cloud (Cl), nimbostratus (Ns) and cumulonimbus (Cb) classes are also represented.

Once classified each measurement set, the second step is to estimate T_m using (8). Since we don't have nor measured T_m, neither measured T_A of ITALSAT channels, we can retrieve T_A at the available radiometer frequencies for testing purposes. To do this, we can basically use the same polynomial model of (8) adapted to our context, i.e. [19]:

$$\hat{T}_m(z=0,\theta,\nu;\hat{c}) = a_0 + \sum_{j=1}^{3}\left\{\sum_{k=1}^{3} a_{jk}\left[A(\theta,\nu_k;\hat{c})\right]^j\right\} \qquad (9)$$

where θ=48.2° and ν_i is equal to 13.0, 23.8 and 31.6 GHz, and ν_k is equal to 18.7, 39.6 and 49.5 GHz. The coefficients a_j have been recomputed, using the same SNEM mid-season dataset. The obtained RMSE values are lower than those in Table II, as 3 predictors are used in (9) instead of 1.

Fig. 3 illustrates the estimated antenna noise temperature at 13.0, 23.8 and 31.6 GHz, derived from the measured slant-path ITALSAT attenuation by means of (9). Measured antenna noise temperatures are also reported for comparison. For the predominantly stratiform event of April 29, the agreement between the estimated and measured antenna noise temperature is fairly good with a trend characterized by an overestimation, especially within the embedded intense portion around minute 220. Overall RMSE's are 2.8, 5.7 and 7.9 K at 13.0, 23.8 and 31.6 GHz, respectively.

The same analysis can be applied to more extreme events, such as that of April 27 [19]. The latter shows higher values of estimated T_A with a well reproduction of the two peaks between minutes 50 and 100. The agreement between the estimated and measured brightness temperature increments is again fairly good with overall RMSE of 7.6, 9.7 and 10.7 K at 13.0, 23.8 and 31.6 GHz, respectively. In both case studies T_A estimates follow very closely the temporal dynamics of multi-frequency antenna noise measurements.

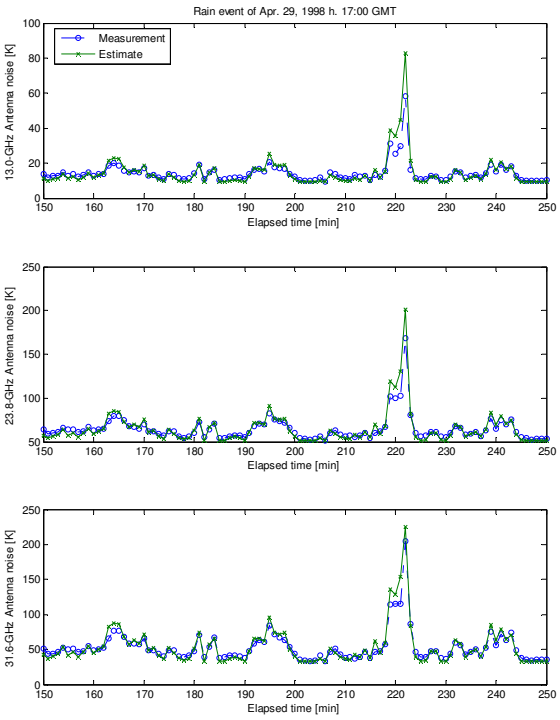

Fig. 3. Estimate of the antenna noise temperature at 13.0, 23.8 and 31.6 GHz from Italsat path attenuation measurements on Apr. 29, 1998 at 17:00 GMT. Measurements are also superimposed.

V. Conclusions

Various applications of a physically-based antenna noise temperature model, named SNEM and described in a previous paper, to some satellite radio-propagation issues have been illustrated. The effective mean temperature of a rainy atmosphere has been formulated for ground-based antennas and the error budget, due to simplifying assumptions usually applied in practice, have been quantified through a numerical sensitivity analysis. One of the most critical parameterization has been found to be the impact of precipitating ice layers, which cannot be neglected at Ka band and, in general, for moderate rain regimes. Precipitation albedo has also revealed to be a crucial parameter when predicting the effective mean temperature, especially for low-to-medium path attenuation. Saturation effects of the effective mean temperature for high rain rate and path attenuation have been also discussed.

Experimental link data have been used to test the proposed physically-oriented prediction methodology by resorting to measurements of the ITALSAT satellite ground-station at Pomezia (Rome, Italy). Combined data from the ITALSAT three-beacon receiver and from a three-channel ground-based microwave radiometer have been investigated. Results have been shown in terms of radiometer antenna noise temperature estimation by using beacon slant-path attenuations as predicting variables. The appreciably good accuracy of the estimates for two rainfall case studies has confirmed the potential of the proposed physically-oriented prediction technique [19].

Acknowledgements

Data from the Italsat station were kindly provided by Dr. A. Martellucci (now at ESA-ESTEC, NL), Dr. E. Fionda and Mr. F. Consalvi of Fondazione Ugo Bordoni (FUB), Rome, Italy.

References

[1] L.J. Ippolito, "Radio propagation for communications", *IEEE Proc.*, vol. 69, pp. 697-727, June 1981.

[2] P.A. Watson and Y.F. Hu, "Prediction of attenuation on satellite-earth links for systems operating with low fade margins", *IEE Proc. - Microw. antennas propagat.*, vol. 141, pp. 467-472, 1994.

[3] A. Dissanyake, J. Allnut and F. Haidara, "A prediction model that combines rain attenuation and other propagation impairments along Earth-satellite paths", *IEEE Trans. Antennas Propagat.*, vol. 45, pp. 1546-1558, 1997.

[4] R.K. Crane, "Prediction of attenuation by rain", *IEEE Trans. Comm.*, vol. 28, pp. 1717-1733, 1980.

[5] E.E. Altshuler and R.A. Marr, "Cloud attenuation at millimeter wavelengths", *IEEE Trans. Antennas Propagat.*, vol. 37, pp. 1473-1479, 1991.

[6] F.S. Marzano and C. Riva, "Cloud-induced effects on long-term amplitude scintillation along millimeter-wave slant paths", *IEEE Trans. Antennas Propagat.*, vol. 51, pp. 880-887, 2003.

[7] M.S. Alouini, S.A. Borgsmiller, and P.G. Steffes, "Channel characterization and modeling for Ka-band very small aperture terminals", *IEEE Proceedings*, vol. 85, n. 6, pp. 981-997, 1997.

[8] B.R. Arbesser-Rastburg and A. Paraboni, "European research on Ka-band slant path propagation," *Proc. of the IEEE*, vol. 85, pp. 843-852, 1997.

[9] A. Ishimaru, and R.L.-T. Cheung, "Multiple-scattering effect on radiometric determination of rain attenuation at millimeter-wavelengths," *Radio Sci.*, vol. 15, pp. 507-516, 1980.

[10] S. Senin, C. Catalan, and E. Vilar, "Influence of sky noise temperature and propagation phase noise on VSAT design at millimeter-wave frequencies", Proc. of 3rd Ka Band Utilization conference, Sorrento (Italy), pp. 401-406, 1997.

[11] F.S. Marzano, C. Di Ciero, P. Ciotti and E. Fionda, "Characterization of ground-based antenna noise temperature due to precipitating clouds from Ku to W band", Proc. of CLIMPARA-2001, Budapest (H), 28-30 May, 2001.

[12] International Telecommunication Union – Radiopropagation (ITU-R), "Radio noise", Recommandation ITU-R P.372-7, pp. 19, Geneva (CH), 2001.

[13] R.K. Crane, X. Wang, D.B. Westenhaver, and W.J. Vogel, "ACTS propagation experiment: experiment design, calibration, and data preparation and archival", *Proc. of the IEEE*, vol. 85, pp. 863-878, 1997.

[14] R. Polonio and C. Riva, "ITALSAT propagation experiment at 18.7, 39.6, and 49.5 GHz at Spino d'Adda: three years of CPA statistics," *IEEE Trans. Antennas and Propagat.*, vol. 46, pp. 631-635, 1998.

[15] G. Brussaard and P.A. Watson, *Atmospheric modelling and millimetre wave propagation*, Chapman & Hall, London (UK), 1995.

[16] F.S. Marzano, E. Fionda, and P. Ciotti, "Simulation of radiometric and attenuation measurements along earth-satellite links in the 10- to 50-GHz band through horizontally-finite convective raincells," *Radio Sci.*, vol. 34, pp. 841-858, 1999.

[17] F.S. Marzano and L. Roberti, "Numerical investigation of intense rainfall effects on coherent and incoherent slant-path propagation at K band and above," *IEEE Trans. Antennas Propagat.*, vol. 41, n. 5, pp. 965-977, 2003.

[18] F.S. Marzano, "Modeling antenna noise temperature due to rain clouds at microwave and millimeter-wave frequencies," *IEEE Trans. Antennas and Propagat.*, vol. 54, pp. 1305-1317, 2006.

[19] F.S. Marzano, "Predicting antenna noise temperature due to rain clouds at microwave and millimeter-wave frequencies," *IEEE Trans. Antennas and Propagat.*, vol. 55, n. 7, pp. 2022-2031, 2007.